

# Investigation of Near-Critical States of Molybdenum by Method of Isentropic Expansion<sup>1</sup>

A. N. Emelyanov,<sup>2,3</sup> A. A. Pyalling,<sup>2</sup> and V. Ya. Ternovoi<sup>2</sup>

---

In this work release isentropes of shocked porous molybdenum were investigated. Samples with an initial porosity  $m = \rho_0/\rho = 1.4$  and 3.1 were studied to achieve near-critical entropy states of metal after shock compression. Compressed samples were expanded into helium with different initial pressures. The brightness temperature of the metal and the helium shock wave velocity were measured with a fast multichannel pyrometer. The helium shock wave velocity was used to determine the final pressure ( $P_S$ ) of expansion of the metal and the velocity of metal expansion ( $W_S$ ). Location of peculiarities on the  $P_S$ - $W_S$  and  $P_S$ - $T_P$  curves of the isentropes gives the location of their entrance into the two-phase region. Estimation of the molybdenum critical temperature and pressure was carried out on the basis of the experimental data.

---

**KEY WORDS:** critical point; isentropic expansion; molybdenum; optical pyrometry; porous sample; shock wave; spinodal.

## 1. INTRODUCTION

Experimental investigations of the thermodynamic properties of matter in near-critical point states of liquid–vapor phase transitions under isentropic expansion of samples, compressed by an one-dimensional plane shock wave, have been performed over a long time period [1]. The majority of experimental data, obtained up to the present time, consists of results of measurements of the velocity of expansion of shocked metal ( $W_S$ ),

---

<sup>1</sup> Paper presented at the Fifteenth Symposium on Thermophysical Properties, June 22–27, 2003, Boulder, Colorado, U.S.A.

<sup>2</sup> Institute of Problem of Chemical Physics of Russian Academy of Sciences, Institutskiy Pr. 18, Chernogolovka 142432, Russia.

<sup>3</sup> To whom correspondence should be addressed. E-mail: emelyanov@ficp.ac.ru

expanded down to a certain measured pressure ( $P_S$ ) [2]. Measurements of the temperature of the expanded metal are also possible by using optical pyrometry in the process of expansion in the helium atmosphere [3–5]. Expanded states with pressures from 0.1 MPa to 2 GPa are accessible, using a striker with an initial velocity of  $6\text{--}7\text{ km}\cdot\text{s}^{-1}$  and an initial pressure of helium changing from  $10^{-3}$  to 10 MPa. Single-shock compressed helium remains transparent up to mass velocities of 10 to  $12\text{ km}\cdot\text{s}^{-1}$  for the experimental basis  $\sim 5\text{ mm}$  (typical thickness of compressed helium layer). This velocity is not sufficient to generate states with a critical entropy value of the liquid–vapor phase transition for initially solid samples of metals with high boiling temperatures [6]. Up to now, this method has been used for determination of critical-point parameters of only lead and tin [3, 4].

To investigate metals with high values of critical entropy, porous samples have been used [2, 7, 8]. In this case, it is possible to reach the near-critical entropy value of the sample by a shock compression wave and the near-critical point states following isentropic expansion, using the striker accelerated up to a velocity of  $\sim 7\text{ km}\cdot\text{s}^{-1}$ . Thus, it is possible to perform pyrometric measurements of the temperatures of the expanded metal. Compressed nickel powder was used as a sample in Refs. 5 and 9. The technique for estimation of the critical-point pressure from pyrometric measurements was similar to that used for solid samples [3, 4]. It is based on the determination of the overheating of metal by hot shocked helium in the vicinity of the critical pressure. An estimation of the critical-point temperature has been determined from the experimental data and from the theoretical estimation of the metal liquid spinodal behavior below the critical point [3, 4, 10].

The main aim of the present study was an estimation of the critical-point parameters (temperature and pressure) of the liquid–vapor phase transition of molybdenum from experiments with isentropic expansion of shocked samples with various initial porosities.

## 2. MEASUREMENTS

### 2.1. Specimens

In the present work flat samples of porous molybdenum (average size of particles  $\sim 10\text{ }\mu\text{m}$ ) with densities  $\rho = 7.2\text{ g}\cdot\text{cm}^{-3}$  (set 1) and  $\rho = 3.3\text{ g}\cdot\text{cm}^{-3}$  (set 2) ( $m = \rho_0/\rho = 1.41$  and  $3.1$ , respectively, where  $\rho$  is the density of the sample and  $\rho_0$  is the density of solid molybdenum, were used. The samples were fabricated in the form of a disk with a diameter of  $15\text{--}20\text{ mm}$  and a thickness of  $0.2\text{--}0.3\text{ mm}$ , manufactured by compression

of raw molybdenum powder (samples with  $m = 1.41$ ), or by agglutination with an alcoholic solution of butyral resin and further annealing (samples with  $m = 3.1$ ; mass percentage of the glue in the sample was 0.05%).

## 2.2. Experimental Setup

The experimental assembly, analogous to that used in Refs. 5 and 6, is presented in Fig. 1. The sample, placed on a stainless steel bottom of the assembly, was shocked by the impact of a steel striker flying with a velocity of  $6.5 \text{ km} \cdot \text{s}^{-1}$  up to a pressure of 225 GPa (set 1) and with a velocity of  $7.2 \text{ km} \cdot \text{s}^{-1}$  up to 146 GPa (set 2). Optical emission was observed with a multichannel optical pyrometer and recorded by a fast oscilloscope "Tektronix" (TDS 5054) with a time resolution of 1 ns. Narrow-band filters in the pyrometer could be used to record signals in the spectral range of 700–1000 nm, with 8 nm width of spectral band. Optical emission from the experimental assembly was transmitted to the pyrometer by optical fibers.

Calculation of the brightness temperature was performed using the results of pre-shot calibration of the fiber-aperture assembly with a reference tungsten ribbon lamp. Using the blackbody ( $\epsilon = 1$ ) emissivity of a

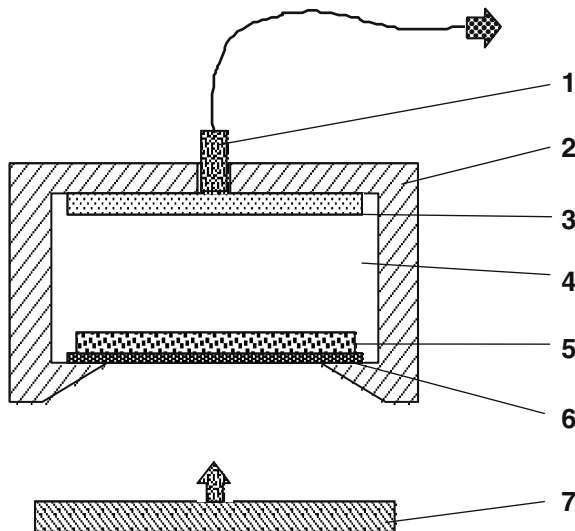


**Fig. 1.** Experimental assembly: 1. optical fiber with aperture; 2. pressurized chamber; 3. glass window; 4. helium under pressure; 5. porous molybdenum sample; 6. steel bottom of assembly; and 7. steel striker.

molybdenum surface, the validity of this approximation was discussed in Ref. 3. The shock wave velocity of helium was measured by the optical base length technique. The particle velocity ( $W_S$ ) and pressure of expansion ( $P_S$ ) were calculated, using a helium equation of state [11] (chemical plasma model).

### 3. RESULTS

In this work two release isentropes of molybdenum with final pressures in the range of 0.02–2 GPa were investigated. The results of measurements of the  $W_S$ – $P_S$  dependence are presented in Fig. 2. The  $W_S$  and  $P_S$  values are presented without regard for deceleration of a sample.

There is good agreement with the predictions of an EOS model [8] and with the experimental data of  $W_S$  at high values of  $P_S$ . An increasing discrepancy of the experimentally measured velocities and theoretical estimations was observed for pressures below the pressure of the entrance of

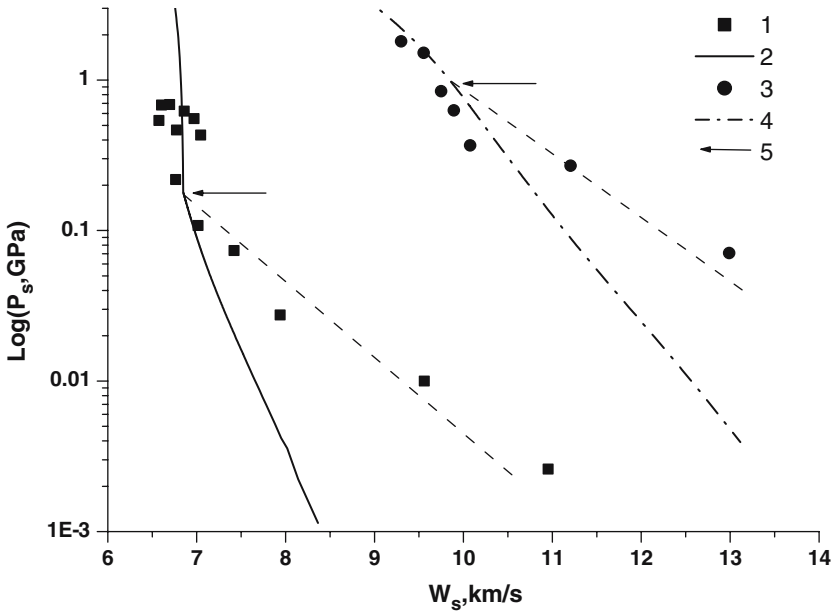


Fig. 2. Pressure-particle velocity graph: 1 – experimental data for porosity  $m = 1.41$ ; 2 – curve-equation of state [6] calculation of release isentrope with initial porosity  $m = 1.41$ ; 3 – experimental data for porosity  $m = 3.1$ ; 4 – curve-equation of state [8] calculation of release isentrope with initial porosity  $m = 3.1$ ; and 5 – pressure of entrance into two-phase region.

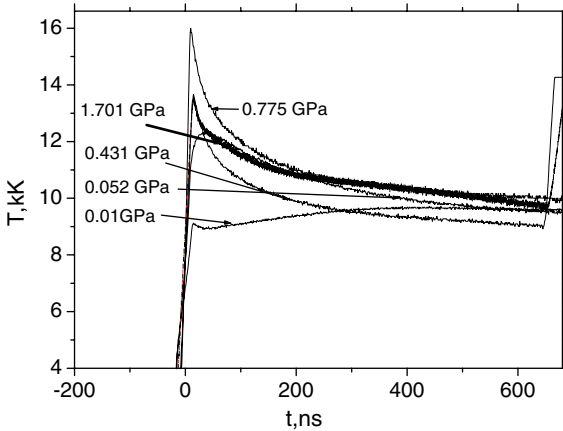


Fig. 3. Typical experimental snapshots at the various final pressures ( $m = 1.41$ ). Emission intensity (at  $\lambda = 805$  nm) already converted to brightness temperature.

the isentrope into the two-phase region. The same behavior was observed in our previous experimental investigations [3–5, 9, 12] and is explained by the formation of a boiling wave. The pressure for entrance of the investigated isentrope into the two-phase region is  $0.18 \pm 0.03$  GPa (set 1).

Registered brightness-temperature profiles at the wavelength  $\lambda = 808$  nm for the experiments with different final expansion pressures are shown in Figs. 3 (set 1) and 4 (set 2). A sharp increase of the temperature up to a peak value is observed in the initial moment; then, after a short interval with a fast drop, a very slow decrease (we can assume it is a constant within 5–10% deviation) is observed. This decreasing temperature profile with intervals of fast and slow decreases can be explained by cooling of the metal's free surface by cold helium. The shocked helium temperature, according to the EOS model [11], was lower than the measured plateau value of temperature ( $T_P$ ) of the expanded molybdenum in all experiments performed.  $T_P$  versus  $P_S$  values for both sets of experiments are presented in Fig. 5. The presented  $T_P$  are values of the temperatures in the final stage of the experiment. The  $P_S$  values are corrected for deceleration of the sample. The calculated shocked helium temperatures, according to the plasma model [11] using the measured shock velocity for both sets of experiments, are also shown in this figure.

The calculation of the molybdenum shock compression according to the model [6] shows that the expansion isentrope of Mo with an initial porosity  $m = 3.1$  (set 2), shock-compressed by the impact of a steel striker with a velocity of  $7.2 \text{ km} \cdot \text{s}^{-1}$ , is close to a critical isentrope. The pressure

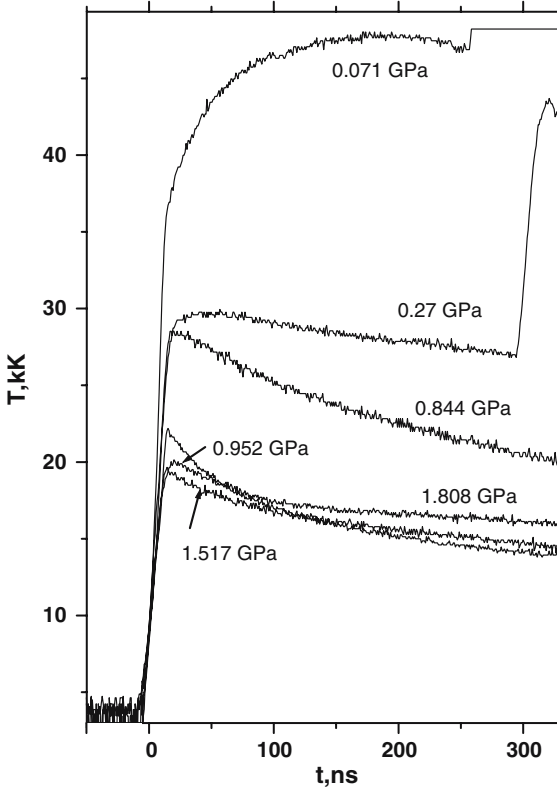
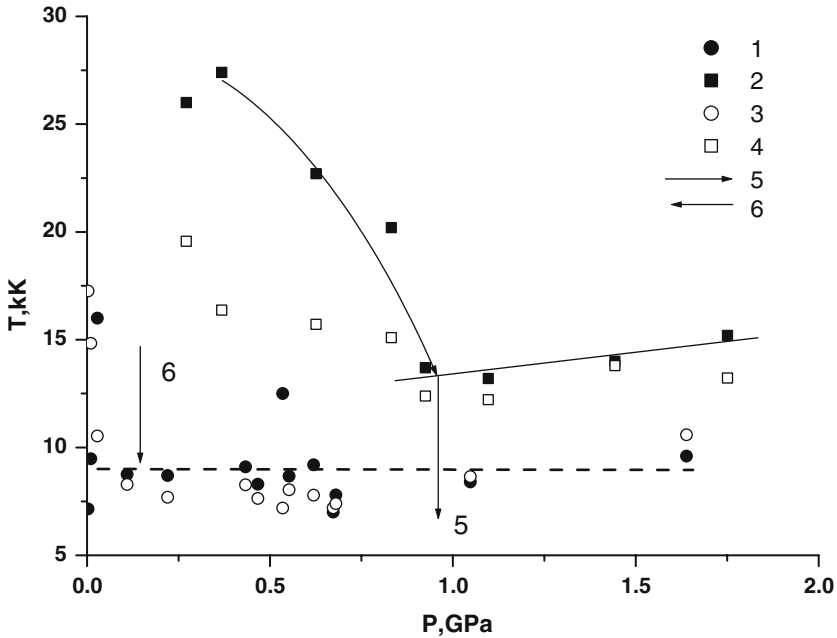


Fig. 4. Typical experimental snapshots at the various final pressures ( $m = 3.1$ ). Emission intensity (at  $\lambda = 805$  nm) already converted to brightness temperature.

of entrance of this isentrope into the two-phase region corresponds to the molybdenum critical-point pressure ( $P_C$ ) within the framework of the experimental pressure uncertainty (10%). According to the model [6] the pressure of the entrance of isentropes into the two-phase region varies from  $0.9 P_C$  to  $P_C$ , for isentropes generated after shock compression of molybdenum ( $m = 3.1$ ) with a steel striker accelerated up to velocities in the range of  $6.8\text{--}9.1 \text{ km}\cdot\text{s}^{-1}$ .

From Fig. 5 it can be seen that the diminishing of  $P_S$  for states in the two-phase region is accompanied by the growth of  $T_P$  values (it is obviously observed for states of set 2). This abnormal growth of temperature needs further explanation.



**Fig. 5.** Pressure-temperature diagram of Mo; plateau value of temperature ( $T_P$ ): 1 – temperature of Mo on plateau  $T_P(m=1.41)$ ; 2 – temperature of Mo on plateau  $T_P(m=3.1)$ ; 3 – helium temperature ( $m=1.41$ ); 4 – helium temperature ( $m=3.1$ ); 5 – critical point; and 6 – pressure of entrance into two-phase region (set 1).

The temperature observed in the experiment is the temperature of the metal–helium boundary [12]. The temperature of molybdenum decreases with a decrease of  $P_S$ , and the temperature of the shocked helium is lower than the temperature of the molybdenum. Thus, the observed plateau temperatures and peak temperatures are significantly higher than the temperatures of molybdenum and helium.

The metal microjets, formed on the sample free surface, can lead to an increase of the observed temperature, but this effect cannot explain the increase of temperature with decreasing pressure.

The fact that the observed temperature is very high and sensitive to the initial pressure of helium, and increases with decreasing pressure leads to the conclusion that this temperature results from the helium in the metal pores. During the initial shock compression of molybdenum, the gas in the pores is also compressed. This compression can be modeled as a multiple shock compression of gas up to the shock pressure of the metal (model of a porous body as a set of foils with helium between them).

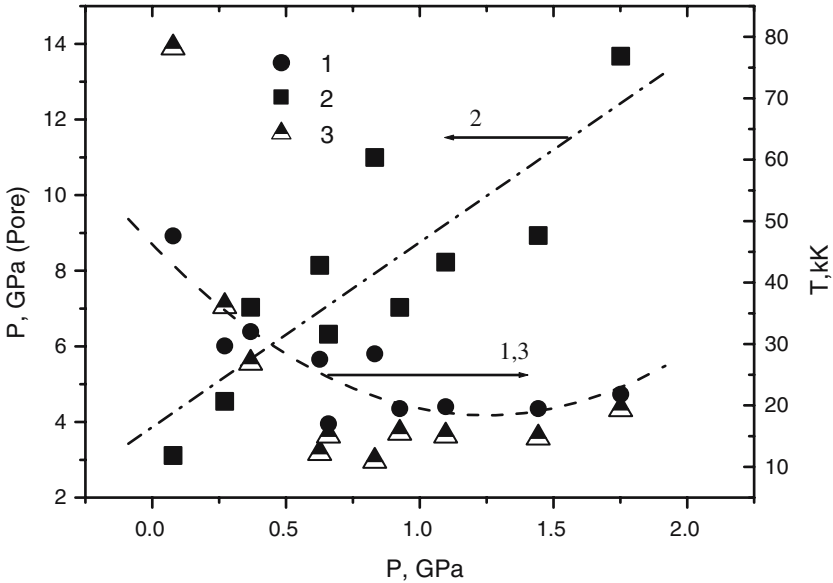


**Fig. 6.** 1 – observed peak temperatures; 2 – calculated pressure in pores corresponding to the observed temperature; and 3 – calculated temperature of helium when compressibility of helium and metal are the same.

The final temperature of helium in such a process is very high, up to 100,000 K, for the experiments performed and shows practically a linear dependence on the initial density of helium. It increases with a decrease of the initial pressure as observed in the experiment. After the shock compression, a release wave traverses the molybdenum isentropically, unloading metal and gas in pores down to  $P_S$ , the final pressure of expansion. The different compressibilities of the gas in pores and the surrounding metal results in different speeds of pressure release within the pores and metal. The process of equalization of pressure results in a perturbation of the metal–gas boundary, an outburst of overheated gas from pores at a free surface of the sample, and leads to a higher value of the observed temperature in comparison with the metal temperature.

In Fig. 6 the maximum peak temperatures observed in experiments of set 2 are plotted versus the final pressures of expansion of molybdenum (curve 1, the right axis). Curve 2 (the left axis) shows the pressures of the isentropically expanded helium, when the temperature of the gas in pores is equal to the observed peak temperature. Despite an increase of the peak temperatures with a decrease of the final pressure of expansion of molybdenum, the corresponding pressure of a gas in the pores decreases.



The dynamic compressibility of the multiple shocked helium in the pores is lower than that of the surrounding compressed metal. After the entrance of a shock wave on the free surface and unloaded wave passes through the molybdenum, the dynamic compressibility of helium increases faster than the compressibility of molybdenum (because the sound velocity in gas decreases faster than the sound velocity in metal after a reduction of pressure). Under a certain pressure the dynamic compressibility of gas becomes higher than that of molybdenum. As a result, the metal unloads faster than the gas in pores, and at some moment, the pressure of the gas becomes higher than the pressure of the surrounding metal. Due to the pressure gradient in the metal during unloading, the high pressure in pores generates forces, outbursting gas from the metal. In Fig. 6 (curve 3, right axis) the temperatures of helium are calculated for pressures at which the dynamic compressibility of helium and molybdenum on isentropes is equal. The good agreement of calculated and experimentally observed peak temperatures demonstrates viability of the proposed model.

The revealed features of the process of generation of near-critical-point states have not allowed the use of the definition of molybdenum critical-temperature approaches given in Refs. 3–5, 9, and 12. The critical temperature and pressure were estimated as the crossing point of interpolation lines of experimental  $T_p$  with  $P_S$  higher and lower than the pressure of an entrance into the two-phase region ( $P_e$ , set 2). Results of various estimations of the critical pressure and temperature [10, 13–17] of molybdenum are reported in Table I. For the most part, the estimations of the critical-point parameters have been obtained using various EOS models [13, 14, 16, 17]. The author of Ref. 16 gives a comprehensive analysis of studies devoted to estimations of the critical-point parameters of metals by various EOS models. In the absence of experimental data in the vicinity of the critical point, the semiempirical EOS models give rough estimates. The only experimental work [15] has been carried out by submicrosecond resistive pulse heating of wire-shaped metallic samples at ambi-

**Table I.** Estimations of Critical-Point Parameters of Molybdenum

$P_c$ (GPa)	$T_c$ (K)	
$0.96 \pm 0.10$	$13,300 \pm 700$	This work
0.533	13,598	Levashov (2000) [16]
0.568	14,300	Seydel et al. (1979) [15]
0.759	10,180	Lomonosov (2000) [17]
0.692	10,780	Martynyuk (1983) [10]
0.175	11,330	Martynyuk and Tamanda (1999) [13]

ent pressure of water. Our estimation of the critical-point temperature is close to the result obtained in Ref. 15. The procedure of pulse pressure determination during the heating process is not understood by us, and the critical-pressure estimation is likely to be underestimated.

#### 4. CONCLUSIONS

The thermodynamic states of porous molybdenum after shock compression and subsequent expansion are investigated. A substantial increase of the measured temperature of the porous samples after shock compression, and the following release at the low initial helium pressure, were observed. A model for multiple shock compression of a gas in metal pores and its subsequent radiation during unloading was suggested. An estimation of the critical-point pressure and temperature for the liquid–gas transition of molybdenum was performed.

#### ACKNOWLEDGMENTS

The authors are indebted to I. V. Lomonosov and V. K. Grjaznov for calculations performed on models [6, 11] and to N. A. Afanas'ev, A. S. Filimonov, and D. N. Nikolaev for invaluable help rendered in preparation and performance of experiments. The work was supported in part by ISTC (Grant No. 2107), and also within the framework of the complex program of scientific researches of the Presidium of the Russian Academy of Science "Thermophysics and the mechanics of high energy density actions." The authors are grateful to the Russian Science Support Foundation for their support.

#### REFERENCES

1. Ya. B. Zeldovich and Yu. P. Raizer, in *Physics of Shock Wave and High Temperature Hydrodynamic Phenomena* (Academic Press, New York, 1966), pp. 592–605.
2. M. V. Zhernokletov, V. N. Zubarev, R. F. Trunin, and V. E. Fortov, in *Experimental Data for Shock Compression and Adiabatic Expansion Condensed Matter at High Density Energy* (Chernogolovka, Russia, 1996), p. 385. (monograph in Russian).
3. V. Ya. Ternovoi, V. E. Fortov, S. V. Kvitov, and D. N. Nikolaev, in *Shock Compression of Condensed Matter*, S. C. Schmidt and W. C. Tao, eds. (AIP Press, Woodbury, New York, 1996), pp. 81–84.
4. V. Ya. Ternovoi, V. E. Fortov, A. S. Filimonov, I. V. Lomonosov, D. N. Nikolaev, and A. A. Pyalling, in *Shock Compression of Condensed Matter*, S. C. Schmidt, D. P. Dandekar, and J. W. Forbes, eds. (AIP Press, Woodbury, New York, 1998), pp. 87–90.
5. V. Ya. Ternovoi, V. E. Fortov, A. S. Filimonov, S. V. Kvitov, D. N. Nikolaev, A. A. Pyalling, and Yu. E. Gordon, *High Temp. High Press.* **34**:73 (2002).

6. V. E. Fortov and I. V. Lomonosov, *J. Pure Appl. Chem.* **69**:893 (1997).
7. A. A. Bakanova, I. P. Dudoladov, and Yu. N. Sutulov, *Zh. Prikl. Mekh. Tekh. Fiz.* **2**:117 (1974) [in Russian].
8. R. F. Trunin, G. V. Simakov, Yu. N. Sutulov, A. B. Medvedev, B. D. Rogozkin, and Yu. E. Fyodorov, *Zh. Exp. Teor. Fiz.* **96**:1024 (1989) [in Russian].
9. D. N. Nikolaev, V. Ya. Ternovoi, A. A. Pyalling, and A. S. Filimonov, *Int. J. Thermophys.* **23**:1311 (2002).
10. M. M. Martynyuk, in *Phase Transitions at Pulse Heating* (Russian University of People Friendship, Moscow, 1999), p. 340 [in Russian].
11. W. Ebeling, A. Foerster, V. E. Fortov, V. K. Gryaznov, and A. Ya. Polishchuk, in *Thermophysical Properties of Hot Dense Plasmas* (Teubner, Stuttgart/Leipzig, 1991), pp. 142–172.
12. A. Pyalling, V. Gryaznov, S. Kvitov, D. Nikolaev, V. Ternovoi, A. Filimonov, V. Fortov, D. Hoffman, C. Stockl, and M. Dornik, *Int. J. Thermophys.* **19**:993 (1998).
13. M. M. Martynyuk and P. A. Tamanda, *High Temp. High Press.* **31**:561 (1999).
14. H. Hess and H. Schneidenbach, *Z. Metallkd.* **87**:79 (1996).
15. U. Seydel, H. Bauhof, W. Fucke, and H. Wadle, *High Temp. High Press.* **12**:635 (1979).
16. P. R. Levashov, in *The Equation of State for Liquid Metals as Soft-Sphere System*, Preprint, CIHT RAS, N1-446-M (2000).
17. I. V. Lomonosov, *Dr. Sc. Thesis* (Inst. Chem. Phys. of Russian Academy of Sciences, Chernogolovka, Russia, 2000) [in Russian].